

*This article has been published in a revised form in Parasitology [http://doi.org/10.1017/S0031182015001997]. This version is free to view and download for private research and study only. Not for re-distribution, re-sale or use in derivative works. © 2017 Cambridge University Press*



**Presence of a isoform of H<sup>+</sup>-pyrophosphatase located in the alveolar sacs of a scuticociliate parasite of turbot and its physiological transcendence**

Journal:	<i>Parasitology</i>
Manuscript ID	PAR-2015-0303
Manuscript Type:	Research Article - Standard
Date Submitted by the Author:	17-Sep-2015
Complete List of Authors:	Mallo, Natalia; University of Santiago de Compostela, Microbiology and Parasitology Lamas, Jesús; University of Santiago de Compostela, Department of Cellular Biology and Ecology de Felipe, Ana; University of Santiago de Compostela, Microbiology and Parasitology De Castro, María; University of A Coruña, Cellular and Molecular Biology Sueiro, Rosa; University of Santiago de Compostela, Microbiology and Parasitology Leiro, Jose; Universidad de Santiago de Compostela, Instituto Análisis Alimentarios;
Key Words:	H <sup>+</sup> -PPase, Philasterides dicentrarchi, alveolar sacs, osmoregulation, turbot

SCHOLARONE™  
Manuscripts

1 Presence of an isoform of H<sup>+</sup>-pyrophosphatase located in the alveolar sacs  
2 of a scuticociliate parasite of turbot and its physiological transcendence

3

4 NATALIA MALLO<sup>1</sup>, JESÚS LAMAS<sup>2</sup>, A. PAULA DE FELIPE<sup>1</sup>, M. EUGENIA DE CASTRO<sup>3</sup>,  
5 ROSANA SUEIRO<sup>1,2</sup>, JOSÉ M. LEIRO<sup>1,\*</sup>

6

7 <sup>1</sup>*Departamento de Microbiología y Parasitología, Instituto de Investigación y Análisis Alimentarios,*  
8 *Universidad de Santiago de Compostela, 15782 Santiago de Compostela, Spain*

9 <sup>2</sup>*Departamento de Biología Celular y Ecología, Facultad de Biología, Universidad de Santiago de*  
10 *Compostela, 15782 Santiago de Compostela, Spain*

11 <sup>3</sup>*Departamento de Biología Celular y Molecular, Facultad de Ciencias, Universidad de A Coruña, 15701*  
12 *A Coruña, Spain*

13

14 SHORT TITLE: **Two isoforms of inorganic pyrophosphatase in *Philasterides***  
15 ***dicentrarchi***

16

17 \*Correspondence to: José M. Leiro, Laboratorio de Parasitología, Instituto de Investigación y Análisis  
18 Alimentarios, c/ Constantino Candeira s/n, 15782, Santiago de Compostela (A Coruña), Spain; Tel:  
19 34981563100; Fax: 34881816070; E-mail: josemanuel.leiro@usc.es

20

21

## 22 SUMMARY

23 H<sup>+</sup>-pyrophosphatases (H<sup>+</sup>-PPases) are integral membrane proteins that couple PPI  
24 energy with an electrochemical gradient across biological membranes and promoted the  
25 acidification of cellular compartments. In eukaryotes organisms, essentially plants and  
26 protozoan parasites, has been described the existence of various types of H<sup>+</sup>-PPases  
27 associated to vacuoles, plasma membrane and acidic Ca<sup>+2</sup> storage organelles called  
28 acidocalcisomes. In this study we achieve to draw, by staining with pH sensitive dye  
29 LysoTracker Red DND 99, the existence of two acidic cellular compartments in  
30 trophozoites of the scuticociliate marine parasite *Philasterides dicentrarchi*: the  
31 phagocytic vacuoles and the alveolar sacs. These compartments also present in its  
32 membranes H<sup>+</sup>-PPase, which could be related with this enzyme promoting acidification  
33 of these cell structures. Furthermore, we demonstrate for the first time that the *P.*  
34 *dicentrarchi* H<sup>+</sup>-PPase is constituted by two isoforms of which one, is probably  
35 generated by alternative splicing, it is localized in the membranes of the alveolar sacs  
36 showing an amino acid motif recognized by the H<sup>+</sup>-PPase-specific antibody PAB<sub>HK</sub>, and  
37 it has a high degree of conservation between aa sequences of different strains of this  
38 ciliate. Gene expression of H<sup>+</sup>-PPase is significantly regulated by variation in salinity,  
39 indicating the role of this enzyme and the alveolar sacs in osmoregulation and salt  
40 tolerance in *P. dicentrarchi*.

41

42 *Keywords:* H<sup>+</sup>-PPase, *Philasterides dicentrarchi*, alveolar sacs, osmoregulation.

43

44

## 45 KEY FINDINGS

- 46 • *Philasterides dicentrarchi* has at least two isoforms of H<sup>+</sup>-PPase
- 47 • The alveolar sacs are acidic structures containing an isoform of the H<sup>+</sup>-PPase
- 48 • The H<sup>+</sup>-PPase of the alveolar sacs is associated with an osmoregulatory function

49

## 50 INTRODUCTION

51 Proton-translocating inorganic pyrophosphatases (H<sup>+</sup>-PPases) are extremely  
52 hydrophobic integral membrane proteins that utilize the energy released upon  
53 hydrolysis of pyrophosphate (PP<sub>i</sub>), that has a high-energy phosphoanhydride bond, to  
54 transport H<sup>+</sup> across the biological membranes against the electrochemical potential  
55 gradient (Maeshima, 2000; Belogurov and Lahti, 2002; Gaxiola *et al.* 2007; Serrano *et al.*  
56 2004). The first discovered H<sup>+</sup>-PPase in membranes isolated from the  
57 photosynthetic bacterium *Rhodospirillum rubrum* (Baltscheffsky *et al.* 1966), later it was  
58 located in homogenates and in higher plant vacuoles (V-H<sup>+</sup>-PPases) as a proton pump  
59 (Karlsson, 1975), and more recently was found in acidocalcisomes of parasitic protozoa  
60 (Scott *et al.* 1998). Although for a long time it was considered that this enzyme was  
61 present only in plants and some photosynthetic bacteria (Drozdowicz *et al.*, 2003.), it has  
62 now been identified in a wide range of organisms including prokaryotes extremophiles,  
63 fungi, some algae and protozoa (Maeshima 2000; Drozdowicz and Rea, 2001). In  
64 plants, V-H<sup>+</sup>-PPases are present, in addition to the vacuole membrane (tonoplast), also  
65 in the plasma membrane (Rea and Poole, 1993; Long *et al.* 1995; Robinson *et al.* 1996).  
66 In protozoans, V-H<sup>+</sup>-PPase is an integral membrane-associated protein that has been  
67 localized, besides to the acidocalcisomes, within the Golgi, plasma membrane, digestive  
68 vacuoles and within a microneme maturation vacuolar compartment of apicomplexans  
69 (Harper *et al.* 2006).

70 The first indication of the existence of the diversity and functional heterogeneity  
71 of V-H<sup>+</sup>-PPases was performed at the plant *Arabidopsis thaliana* observing the presence  
72 of two distinct categories of the enzyme: the AVP1 and AVP2 that, after the phylogenetic  
73 analyses with other V-H<sup>+</sup>-PPases, showing that AVP2, rather than being an isoform of  
74 AVP1, is but one representative of a novel category of AVP2-like (type II) V-PPases  
75 that coexist with AVP1-like (type I) V-H<sup>+</sup>-PPases not only in plants, but also in  
76 apicomplexan protists such as the malarial parasites (Drozdowicz *et al.* 2000). Although  
77 there is a clear evidence for a wide occurrence of V-H<sup>+</sup>-PPase genes in ciliates  
78 hymenostomatids, peritrichs and hypotrichs (Pérez-Castiñeira *et al.* 2002); however,  
79 until recently has only been shown the presence of V-H<sup>+</sup>-PPase activity in the  
80 scuticociliate parasite of turbot *Philasterides dicentrarchi* (Mallo *et al.* 2015).

81 More specifically, in this work we report the results of a study that show for the  
82 first time the existence of a sequence variant in genes encoding two isoforms of H<sup>+</sup>-  
83 PPase in *P. dicentrarchi*. One of these isoforms of the enzyme are predominant located  
84 in flat cortical sacs, designed “alveolar sacs” in Ciliophora, and their gene expression  
85 were modulated for the salt concentration.

86

## 87 MATERIALS AND METHODS

### 88 *Parasites and experimental animals*

89 Specimens of *P. dicentrarchi* (isolates B1, C1, D2, D3, I1, S1, P1; Iglesias *et al.* 2001;  
90 Budiño *et al.* 2011) were collected under aseptic conditions from ascitic fluid removed  
91 from the intraperitoneal cavity of experimentally infected turbot, *Scophthalmus*  
92 *maximus*, as previously described (Paramá *et al.* 2003). The ciliates were cultured at 21°C  
93 in complete sterile L-15 medium as previously described (Iglesias *et al.* 2003). In order  
94 to maintain the virulence of the ciliates, fish were experimentally infected every 6

95 months by intraperitoneal injection of 200  $\mu$ L of sterile physiological saline containing  
96  $5 \times 10^5$  trophozoites, and the ciliates were recovered from ascitic fluid and maintained in  
97 culture as described above

98 Turbot, of approximately 50 g body weight, were obtained from a local fish  
99 farm. The fish were kept in 250-L tanks with recirculating, aerated sea water at 14 °C,  
100 subjected to a photoperiod of 12L:12D, and fed daily with commercial pellets  
101 (Skretting, Burgos, Spain). Fish were acclimatized to laboratory conditions for 2 weeks  
102 before the experiments were started.

103 Eight to 10- week-old ICR (Swiss) CD-1 mice initially supplied by Charles  
104 River Laboratories (USA) were bred and maintained in the Central Animal Facility of  
105 the University of Santiago de Compostela (Spain) following the criteria of protection,  
106 control, care and welfare of animals and the legislative requirements relating to the use  
107 of animals for experimentation (EU Directive 86/609 / EEC), the Declaration of  
108 Helsinki, and/or the Guide for the Care and Use of Laboratory Animals as adopted and  
109 promulgated by the US National Institutes of Health (NIH Publication No. 85-23,  
110 revised 1996). The Institutional Animal Care and Use Committee of the University of  
111 Santiago de Compostela approved all experimental protocols.

112

113 *PCR, RT-PCR, RT-qPCR*

114 *P. dicentrarchi* DNA was purified with DNAeasy Blood and Tissue Kit (Qiagen)  
115 following the manufacturer's instructions. DNA was analyzed to estimate its quality,  
116 purity and concentration by  $A_{260}$  measurement in a NanoDrop ND-1000  
117 Spectrophotometer (NanoDrop Technologies, USA.)

118 Total RNA was isolated of *P. dicentrarchi* trophozoites with a NucleoSpin RNA  
119 kit (Macherey-Nagel, Düren, Germany), following the manufacturer's instructions after

120 24 hours of trophozoites incubation in culture media with different saline  
121 concentrations: 4, 8 y 37 %. After RNA purification, quality, purity and concentration  
122 were measured with NanoDrop ND-1000 Spectrophotometer (NanoDrop Technologies,  
123 USA). For the cDNA synthesis (25  $\mu$ L/reaction mixture), it was employed a reaction  
124 mix containing: 1.25  $\mu$ M random hexamer primers (Promega), 250  $\mu$ M each  
125 deoxynucleoside triphosphate (dNTP), 10mM dithiothreitol (DTT), 20U of RNase  
126 inhibitor, 2.5mM  $MgCl_2$ , 200U of MMLV (Moloney murine leukemia virus reverse  
127 transcriptase (Promega) in 30mM Tris and 20mM KCl (pH 8.3) and 2  $\mu$ g of sample  
128 RNA. PCR (for DNA and cDNA amplification) was executed with gene-specific  
129 primers for the  $H^+PPase$  gene: forward/reverse primer pair (FPiPh/RPiPh) 5'-  
130 CGGGACCAGAGGTATCTTTTA-3' / 5'-ATTGATGTCAACGCCCCCTT-3'; and  
131 forward/ reverse primer pair (F1qPiPh/R1qPiPh) 5'-GCCTACGAAATGGTCGAAGA-  
132 3' / 5'-GCATCGGTGTATTGTCCAGA-3' for quantitative real-time reverse  
133 transcriptase PCR (RT-qPCR). In parallel, a PCR with primers for the  $\beta$ -tubulin gene  
134 (forward/reverse primer pair, 5'-ACCGGGGAATCTTAAACAGG-3' / 5'-  
135 GCCACCTTATCCGTCCACTA-3') was done to use  $\beta$ -tubulin as a reference gene  
136 (RT-qPCR). For the design and optimization of the primer sets, Primer 3Plus program  
137 was utilized, based on default parameters. PCR mixtures (25  $\mu$ L) contained PCR  
138 reaction buffer (10 mM Tris-HCl, 50 mM KCl, 1.5 mM  $MgCl_2$ , pH 9.0), 0.2 mM of  
139 each deoxynucleoside triphosphate (dNTPs, Roche), 0.4 mM of each primer, 3 units of  
140 recombinant Taq polymerase (NZY Taq DNA polymerase, Nzytech, Portugal) and 50  
141 ng of genomic DNA or 2 $\mu$ L of cDNA. The reactions were run in automatic  
142 thermocycler (Biometra, Germany) as follows: initial desnaturing at 94°C for 5 min;  
143 then 35 cycles at 94°C for 30 s, 57°C for 45 s, and 72°C for 1 min; and finally a 7 min  
144 extension phase at 72°C. qPCR mixtures (10  $\mu$ L) contained 5- $\mu$ L Maxima SYBR green



145 qPCR Master Mix (Thermo Scientific), the primer pair at 300 nM, 1µL of cDNA, and  
146 RNase-DNase-free water. qPCR was developed at 95°C for 5 min, followed by 40  
147 cycles at 95°C for 10 s and 60°C for 30 s ending with a melting-curve analysis at 95°C  
148 for 15 s, 55°C for 15 s, and 95°C for 15 s. The specificity and size of PCR products  
149 were confirmed by 4% agarose gel electrophoresis. All qPCRs were performed in an  
150 Eco Real-Time PCR system (Illumina). Relative quantification of gene expression was  
151 determined by the  $2^{-\Delta\Delta C_t}$  method (Livak K.J., *et al.* 2001) by using software conforming  
152 to MIQE (minimum information for publication of quantitative real-time PCR  
153 experiments) guidelines (Bustin *et al.* 2009)

154

#### 155 *Production of recombinant H<sup>+</sup>-PPase of P. dicentrarchi in yeast cells*

156 *P. dicentrarchi* RNA was purified with a NucleoSpin RNA kit (Macherey-Nagel,  
157 Düren, Germany), following the manufacturer's instructions and cDNA synthesis was  
158 performed as indicated in the previous section. The PCR was carried out with gene-  
159 specific primers designed from a partial sequence of the H<sup>+</sup>-PPase of *P. dicentrarchi*  
160 (Mallo *et al.* 2015) (forward/reverse primer pair 5'-  
161 AAAGAAGAAGGGGTACCTTTGGATAAAAGAattgatgtcaacgccccctt-3' / 5'-  
162 TGGGACGCTCGACGGATCAGCGGCCGCTTAGTGGTGGTGGTGGTGGTGGggac  
163 cagaggtatctttta-3'). These primers were designed and optimized by means of the  
164 *Saccharomyces* Genome Database (<http://www.yeastgenome.org/>) including a  
165 hybridization region with the yeast YEpFLAG-1 (Eastman Kodak Company) plasmid  
166 and a poly His region (lower case letters correspond with the gene annealing zone).  
167 PCR reaction was developed initially at 95 °C for 5 min, and then for 30 cycles of 94 °C  
168 for 1 min, 55 °C for 1.5 min and 72 °C for 2 min. After the 30 cycles, a 7-min extension  
169 phase at 72 °C was carried out. The PCR products were purified using Gene Jet PCR

170 Purification Kit (Fermentas, Life Sciences) according with the manufacturer's  
171 instructions.

172 Purified PCR products were cloned in YEpFLAG-1 (Eastman Kodak Company)  
173 yeast expression vector, a plasmid that carries a TRP1 gene that completes the  
174 auxotrophy for the tryptophan for the host yeast (López-López *et al.* 2010).

175 Linearized plasmid YEpFLAG-1 by digestion with *EcoRI* and *Sall* (Takara) was  
176 used to transform *Saccharomyces cerevisiae* cells (strain BJ 3505) by the lithium  
177 acetate procedure (Ito *et al.* 1983). The procedure involves co-transformation of yeast  
178 cells with the linearized empty plasmid and the PCR-generated DNA fragment so that a  
179 recombination process occurs within the cell yielding a plasmid bearing the desired  
180 insert. Positive colonies were selected using complete medium without tryptophan (CM-  
181 Trp) containing glucose (20g/L), Yeast Nitrogen Base without amino acids medium  
182 (Sigma-Aldrich) adenine (40mg/L) and amino acids (histidine, leucine, tyrosine,  
183 40mg/L each; arginine, methionine, threonine 10mg/L each; isoleucine and  
184 phenylalanine 60mg/L each and lysine 40mg/L).

185 Plasmid DNA was then extracted with Easy Yeast Plasmid Isolation Kit  
186 (Clontech) following the manufacturer's instructions. The purified and cloned DNA  
187 fragment was subjected to sequencing analysis (Sistemas Genómicos, Spain).

188 Recombinant protein of H<sup>+</sup>-PPase of *P. dicentrarchi* was purified from  
189 transformed *Saccharomyces cerevisiae* cultures, after 72h in modified Yeast Peptone  
190 High Stability Expression Medium (YPHSM) containing 1% glucose, 3% glycerol, 1%  
191 yeast extract, and 8% peptone, at 30°C in Erlenmeyer flasks filled with 20% volume of  
192 culture medium at 250 rpm (López-López *et al.* 2010). As inoculum, a suitable volume  
193 of a pre-culture was added to obtain an initial OD<sub>600</sub> of 0.1. The cell suspension was  
194 centrifuged at 7500g for 15 min and the cleared supernatant was purified by

195 immobilized metal affinity chromatography on a pre-charged Ni-Sepharose HiTrap  
196 column (ÄKTAprime plus, GE Healthcare Life Sciences). The column was initially  
197 equilibrated with 25 mL of binding buffer (20 mM sodium phosphate, 0.5 M NaCl, 20  
198 mM imidazole, pH 7.4). After the equilibration 100mL of culture medium were charged  
199 through the column and finally, the protein bound to the column was eluted in 10 mL of  
200 elution buffer (20mM sodium phosphate, 0.5 M NaCl, 250 mM imidazole, pH 7.4)  
201 (Mallo *et al.* 2015) Fractions from the elution were analyzed by 12.5% SDS-PAGE and  
202 dialyzed overnight in 2 L of bidistilled water. The dialyzed sample was concentrated in  
203 an Amicon Ultra centrifugal filter device (Millipore, USA) with a 10-kDa cut-off  
204 membrane. The final protein concentration was calculated by the Bio-Rad Protein  
205 Assay, which is based on the Bradford assay (Bradford, 1976).

206

#### 207 *Peptide synthesis*

208 A peptide of 17 amino acids long corresponding to domain HKAAVIGDTIGDPLKDT  
209 (PAB<sub>HK</sub>) of the *P. dicentrarchi* H<sup>+</sup>-PPase were synthesized and conjugated to keyhole-  
210 limpet hemocyanin (KLH), a carrier protein, to assure maximum immunogenicity  
211 (ProteoGenix, France). A cysteine amino acid was added to two sequences to allow  
212 conjugation to KLH. The peptide were synthesized and conjugated to KLH by coupling  
213 agent sulfo-SMCC at a yield of 10-20 mg having >85% purity, lyophilized and stored at  
214 -20°C until use.

215

#### 216 *Immunization and serum extraction*

217 A group of five ICR (Swiss) CD-1 mice were immunized by i.p. injection with 200µL  
218 per mouse of a 1:1 (v/v) mixture of Freund complete adjuvant (Sigma-Aldrich) and a  
219 solution containing 500 µg of purified recombinant H<sup>+</sup>-PPase and 400 µg of synthetic

220 peptide in PBS. The same dose of purified protein and peptide was prepared in Freund's  
221 incomplete adjuvant and injected i.p in mice 15 and 30 days after the first  
222 immunization. The mice were bled via retrobulbar venous plexus 7 days after the  
223 secondary immunization (Piazzon *et al.* 2011). The blood was left to coagulate  
224 overnight at 4° C before the serum was separated by centrifugation (2000 × g for 10  
225 min), mixed 1:1 with glycerol and stored at −20°C until use. In some experiments, a  
226 commercial rabbit polyclonal serum against KLH-conjugated synthetic peptide derived  
227 from *Arabidopsis thaliana* V-PPase, (anti-AVP1; UniProt P311414; Agrisera, Sweden)  
228 was also used.

229

### 230 *Western-blot analysis*

231 Ciliate membrane-associated proteins (MAPs) were extracted by phase separation in  
232 Triton X-114 solution (Bordier, 1981), by a previously described method (Mallo *et al.*  
233 2013). Specifically, 10<sup>7</sup> cells were resuspended in 1 ml of ice-cold 10 mM Tris–HCl  
234 buffer, pH 7.5, to which 1 ml of ice-cold extraction buffer (300 mM NaCl, 20 mM Tris–  
235 HCl, pH 7.5, 2% Triton X-114) was subsequently added. The cytoskeletal elements  
236 were eliminated by centrifugation at 16000 x g for 10 min at 4 °C. The supernatant was  
237 then transferred to 1.5 ml Eppendorf tubes, which were heated for 5 min at 37 °C. At the  
238 end of this period, the solution became cloudy as a result of condensation of detergent  
239 micelles. The sample was then placed in 0.5 ml Eppendorf tubes (200  $\mu$ l/tube)  
240 containing 300  $\mu$ l of sucrose cushion (6% sucrose, 150 mM NaCl, 10 mM Tris–HCl, pH  
241 7.5, 0.06% Triton X-114). The detergent and aqueous phases were separated by  
242 centrifugation at 300 g for 4 min at room temperature. The resulting supernatants on the  
243 sucrose cushion of each tube were extracted carefully and mixed in new 1.5 ml  
244 Eppendorf tubes. The extraction process was repeated by adding sufficient Triton X-114

245 to the aqueous mixture to obtain a final concentration of 0.5%. The mixture was re-  
246 heated at 37 °C for 5 min. Once micellar condensation had taken place, the mixture was  
247 distributed among the original Eppendorf tubes containing the sucrose cushion and the  
248 detergent phase separated in the first extraction. The tubes were then recentrifuged at  
249 300 g for 4 min at room temperature. The resulting supernatant was discarded and the  
250 proteins contained in the detergent phase were precipitated, by adding 9 volumes of cold  
251 acetone, resuspended, by vortexing, and finally incubated for 30 min on ice. The  
252 precipitated membrane proteins were then collected by centrifugation at 16000 g for 15  
253 min at 4 °C and dried in a speed vacuum concentrator (MiVac, GeneVac, UK). Finally,  
254 the extracts obtained were resuspended in 10 mM Tris-HCl, pH 7.5, and stored at -80  
255 °C until use. The protein concentration of preparation was determined by Bradford  
256 assay.

257 Samples from MAPs were separated under non-reducing conditions by linear  
258 SDS-PAGE 12.5 % gels (Piazzon *et al.* 2008). After the electrophoresis, the gels were  
259 stained with Thermo Scientific GelCode Blue Safe Protein Stain (Thermo Fisher, USA)  
260 to determine qualitatively the protein bands. In parallel, a gel was submitted to  
261 immunoblotting at 15 V for 35 min to Immobilon-P transfer membranes (0.45  $\mu$ m;  
262 Millipore, USA) in a trans-blot SD transfer cell (Bio-Rad, USA) with the transference  
263 buffer (48 mM Tris, 29 mM glycine, 0.037% SDS and 20% methanol, pH 9.2). The  
264 membrane was washed with Tris buffer saline (TBS; 50 mM Tris, 0.15 M NaCl, pH  
265 7.4) and immediately stained with Ponceau S to verify transfer. After membrane  
266 destaining with bidistilled water, a blocking solution containing 0.2% Tween 20 and 3%  
267 BSA with TBS was added and the membrane was incubated for 1.5 h at room  
268 temperature. Then, it was washed in TBS and incubated overnight with anti-PAB<sub>HK</sub> at  
269 1:100 dilutions, at 4°C. Subsequently; the membrane was washed with TBS and

270 incubated with rabbit anti-mouse IgG (Dakopatts; dilution 1:6000) for 1 h at room  
271 temperature. Once the membrane was washed 5 times for 5 min with TBS, it was  
272 incubated for 1 min with enhanced luminol-based chemiluminiscent substrate (Pierce  
273 ECL Western Blotting Substrate, Thermo Scientific, USA) and then visualized and  
274 photographed with a FlourChem® FC2 imaging system (Alpha Innotech, USA).

275

276 *Immunofluorescence, Immunoelectron microscope and fluorescent stain with pH-*  
277 *sensitive dye*

278 For immunolocalization of H<sup>+</sup>-PPase isoforms, an immunofluorescence assay was  
279 performed following the protocol described previously (Mallo *et al.* 2015). Briefly,  
280 5x10<sup>6</sup> ciliates were centrifuged at 750 x g for 5 min, washed twice with Dulbecco's  
281 phosphate buffered saline (DPBS, Sigma Aldrich) and fixed for 5 min in a solution of  
282 4% formaldehyde in DPBS. Following fixation, ciliates were washed twice with DPBS,  
283 resuspended in a solution containing 0.1% Triton X-100 (PBT) for 3 min and then  
284 washed twice with DPBS. Ciliates were then incubated with 1% bovine serum albumin  
285 (BSA) for 30 min. After blocking, ciliates were incubated at 4°C overnight with a  
286 solution containing 1:100 dilutions of anti-H<sup>+</sup>-PPase form recombinant yeast antibody  
287 and anti-PAB<sub>HK</sub>. Then, ciliates were washed 3 times with DPBS followed by 1 h  
288 incubation, at room temperature; with a 1:100 dilution of FITC conjugated rabbit/goat  
289 anti-mouse/rabbit IgG-FITC antibody (Sigma). After three in DPBS, the samples were  
290 double stained with 0.8 mg/mL 4', 6-diamidino-2-phenylindole (DAPI; Sigma-Aldrich)  
291 in DPBS for 15 min at room temperature (Paramá *et al.* 2007). After three washes with  
292 DPBS samples were mounted in PBS-glycerol (1:1) and visualized by fluorescence  
293 microscopy (Zeiss Axioplan, Germany) and/or confocal microscopy (Leica TCS-SP2,  
294 LEICA Microsystems Heidelberg GmbH, Mannheim, Germany).

295 For immunoelectron microscopy,  $5 \times 10^6$  ciliates from cultures in exponential  
296 growth phase were centrifuged at  $750 \times g$  for 5 min and washed in two changes of  
297 Sørensen buffer (SB; 0.1 M sodium/potassium phosphate buffer, pH 7.3) at room  
298 temperature (RT). The resulting pellet were fixed for 60 min in 4% paraformaldehyde  
299 and 0.1% glutaraldehyde in SB at 4°C. After the fixation, samples was washed in two  
300 changes of SB (10 min each) and incubated with 0.02 M glycine in SB for 10 min at  
301 RT. Ciliates were dehydrated in series of pre-cooled ethanol solutions (30, 50, 70, 80,  
302 96 and 100% of 10 min each). After dehydration, the pellet were included in a mix of  
303 ethanol and resin (LR White uncatalized, Santa Cruz Biotechnology, USA;  
304 [Philimonenko et al. 2002](#)) 2:1 for 20 min and pure resin for 2 h. Samples were infiltrate  
305 overnight with fresh resin at 4°C. The next day, a new exchange of fresh resin was made  
306 and allowed to polymerize at 65 °C in vacuum for 48h. Thin sections (80 nm thick)  
307 were cut with a diamond knife on a Reichert Ultracut E (Leica Microsystems AG,  
308 Germany). Thin sections were collected on 300 mesh nickel grids (Sigma-Aldrich) and  
309 was blocked by preincubation with 10% normal goat serum (NGS) in PBS-10%  
310 albumin and 0.1% Tween-20 (PBTB) for 30 min at RT. The sections were incubated for  
311 1 h with a primary polyclonal antibody anti-AVP1 diluted in PBTB at 1:100 dilution,  
312 washed in PBS-albumin, and incubated with 10 nm gold-labeled goat anti-rabbit IgG  
313 (Sigma) at 1:50 dilution for 60 min. Finally the sections were washed in distilled water,  
314 stained with uranyl acetate and lead citrate, and observed with a JEOL-JEM-2010  
315 transmission electron microscope operating at 120 kV (JEOL, Japan). Controls were  
316 carried out using a non-related antibody or incubation in the presence of the secondary  
317 antibody only.

318 For identification of the acidic compartments on trophozoites of *P. dicentrarchi*  
319 we used a fluorescent stain assay with pH-sensitive dye LysoTracker Red DND-99.

320  $5 \times 10^5$  ciliates were centrifuged at 700 x g for 5 min and washed twice with PBS  
321 followed by a 10 min staining with 75 nM LysoTracker Red DND-99 (Lifetechnologies)  
322 solution. After staining, ciliates were observed in a fluorescence microscopy with an  
323 excitation filter BP 546 nm, dichroic mirror FT 580 nm and emission filter LP 590 nm.

324

### 325 *Bioinformatic and statistical analysis*

326 The aminoacid sequences obtained for the H<sup>+</sup>-PPase gene were aligned with the  
327 multiple alignments Clustal Omega program (Sievens *et al.* 2011). Genetic distances  
328 were calculated to quantify sequences divergences among isolates by use of Kimura's  
329 (1980) two-parameter model, as implemented in MEGA versión 6.0 (Tamura *et al.*  
330 2013). Phylogenetic tree were constructed with the MEGA programme, by the  
331 neighbour-joining (NJ) method applied to the Kimura two-parameter correction model  
332 (Kimura 1980) by bootstrapping with 1000 replicates (Felsenstein, 1985).

333 The results are expressed as means  $\pm$  standard error of the mean (S.E.M.). The  
334 data were examined by one-way analysis of variance (ANOVA) followed by Tukey–  
335 Kramer test for multiple comparisons, and differences were considered significant at  
336  $\alpha = 0.05$ .

337

## 338 RESULTS

### 339 *Cellular localization of H<sup>+</sup>-PPase of P. dicentrarchi in acidic compartments*

340 Initially we cloned a cDNA fragment encoding 169 aa located between positions 305  
341 and 474 of the aminoacid sequence of the H<sup>+</sup>-PPase (GenBank accession AHH28243)  
342 containing domain HKAVIGDTIGDPLKDTS in yeast expression vector YepFlag-1.  
343 The mouse anti-H<sup>+</sup>-PPase polyclonal antibodies generated following immunization with  
344 the recombinant protein fragment, produces intense fluorescent staining of vacuoles



345 located on the back half part of trophozoites and alveolar sacs located under the plasma  
346 membrane (Fig. 1A).

347 Incubation of trophozoites of *P. dicentrarchi* with pH sensitive dye LysoTracker  
348 Red DND-99, produces an intense staining in the vacuoles and in the alveolar sacs (Fig.  
349 1B).

350

351 *Immunohistochemical pattern of the H<sup>+</sup>-PPase when polyclonal antibodies PAB<sub>HK</sub>*  
352 *were used*

353 Indirect immunofluorescence studies using a mouse polyclonal antibody generated  
354 against a KLH-conjugated synthetic peptide of the conserved amino acid domain  
355 HKAAVIDTIGDPLKDT (PAB<sub>HK</sub>; Fig. 2A) and the polyclonal antibody anti-AVP, a  
356 KLH-conjugated synthetic peptide derived from *Arabidopsis thaliana* V-PPase (Fig.  
357 3B), reveal a unique labeling on the surface of the parasite appreciate clear punctate  
358 staining pattern in the trophozoites of *P. dicentrarchi*. In immunoelectron microscopy  
359 using the polyclonal antibody anti-AVP1 clearly shows specific labeling in the  
360 membranes of the alveolar sacs (Fig. 3 C-D).

361

362 *Sequence characteristics of H<sup>+</sup>-PPase isoforms*

363 To investigate the possible existence of various types of H<sup>+</sup>-PPase in *P. dicentrarchi*  
364 located in the posterior vacuoles and in the alveolar sacs, we amplified a fragment of  
365 this gene by PCR and have also generated several cDNA from RNA using the pair of  
366 primers FPiPh/RPiPh. In Figure 3A, the results of nucleotide sequence amplified by  
367 PCR corresponding to an partial open reading frame (ORF) of H<sup>+</sup>-PPase gene and its  
368 amino acid translation are shown. When analyzing on agarose gel 4% the DNA  
369 fragment amplified with primers FPiPh / RPiPh, the appearance of a single band of 558

370 nucleotides in size was observed; however, when a cDNA is generated from total RNA  
371 by RT-PCR and amplified with the same primers, two bands were obtained, one with an  
372 identical size to that obtained after DNA amplification (558 nucleotides) and a second  
373 band of 495 nucleotides (Fig. 3A). The sequencing of of the two bands obtained by RT-  
374 PCR showed that the nucleotide sequence of the larger fragment corresponded exactly  
375 to the sequence obtained by PCR from genomic DNA, whereas the sequencing of the  
376 minor band showed the disappearance of 63 nucleotides which is located in the largest  
377 band. After translation to aa of the two amplified fragments by RT-PCR, shows that the  
378 lower band produces a protein containing the domain complete  
379 HKAAVIGDTIGDPLKDTS, while the largest band generates a protein with this  
380 fragmented domain, containing an internal sequence of 21 amino acids (Fig. 3A).

381 Polyclonal antibodies generated in mice after immunization with the synthetic  
382 peptide corresponding to domain PAB<sub>HK</sub>, recognized on MAPs in Western blot a single  
383 protein band of approximately 60 kD (Fig. 3B).

384

385 *Phylogenetic analysis of H<sup>+</sup>-PPases in several strains of P. dicentrarchi*

386 To determine the degree of phylogenetic evolution between isolates of *P. dicentrarchi*,  
387 we amplified by PCR the DNA of seven isolates using the primers pair FPiPh / RPiPh.  
388 After obtaining the nucleotide sequence of each isolate and its translation into aa, was  
389 carried out a multiple alignment of the amino acid sequences using the Clustal Omega  
390 program, showing a very high degree of conservation between aa sequences of the  
391 isolates analyzed (Fig. 4A). This high level of conservation in aa sequences results in  
392 the existence of a low genetic distance between isolates and, when the phylogenetic tree  
393 using the NJ method is constructed, it is noted that five isolates have 100% homology  
394 (I1, B1, D3, P1 and S1 isolates), whereas D2 and C1 constitute two phylogenetically  
395 different groups (Fig. 4B).

396

397 *Effect of salt concentration on the expression of H<sup>+</sup>-PPase*

398 The assays on the expression levels of RNA corresponding to the H<sup>+</sup>-PPase of *P.*  
399 *dicentrarchi* trophozoites cultivated in a saline medium containing different  
400 concentrations of NaCl: between 4, 8 and 37 ‰, are shown in Fig.5. Relative mRNA  
401 levels, quantified by qPCR, of H<sup>+</sup>-PPase remain unchanged at NaCl concentrations  
402 between 8 and 37 ‰; however when the medium contains low concentrations of NaCl  
403 (such as 4‰), a significant increase in the expression of H<sup>+</sup>-PPase, relative to levels  
404 obtained in ciliates then incubated at concentrations of NaCl between 8 and 37 ‰ (Fig.  
405 5).

406

407 DISCUSSION

408 H<sup>+</sup>-PPases are enzymes that translocates H<sup>+</sup> across a membrane by using potential  
409 energy liberated on hydrolysis of the phosphoanhydride bond of inorganic phosphate  
410 (Read and Poole, 1993). They are widely distributed among land plants and have been  
411 found in several of protozoan parasites including the scuticociliate parasite of turbot, *P.*  
412 *dicentrarchi* (Mallo *et al.* 2015). In eukaryotes, H<sup>+</sup>-PPases are associated to certain  
413 acidic compartments of the endomembrane system, namely, the vacuole and lysosomes  
414 of plant cells and the acidocalcisomes of trypanosomatids and apicomplexans  
415 protozoan (Pérez-Castiñeira *et al.* 2002; Scott and Docampo, 2000; Docampo *et al.*  
416 2005). Some functions of the acidocalcisomes are the storage of cations, Ca<sup>2+</sup>  
417 homeostasis, maintenance of intracellular pH homeostasis and osmoregulation (Moreno  
418 and Docampo, 2009). In parasitic protozoans, acidocalcisomes also interact with other  
419 organelles as the contractile vacuole and other vacuoles associated with the  
420 endosomal/lysosomal pathway (Moreno and Docampo, 2009; Docampo *et al.* 2010). In

421 ciliates, such as *Paramecium caudatum*, has been described acidification of phagocytic  
422 vacuoles occurs through fusion nonlysosomal vesicles, named acidosomes, with the  
423 newly released vacuoles and these vesicles accumulate neutral red as well as acridine  
424 orange, two observations that demonstrate their acid content (Allen and Fok, 1983).  
425 Sequencing of the whole genome of several species of ciliates enable the identification  
426 of genes encoding the V-ATPase, a proton pump that drives  $H^+$  across membranes, and  
427 that is crucial as an acidifier of food vacuoles (Plattner, 2010); however, although there  
428 is evidence of the existence of  $H^+$ -PPases in ciliates, since there are several sequences  
429 deposited in nucleotide databases (eg. *Tetrahymena thermophila*, GenBank accession  
430 XM\_001011583; *Tetrahymena pyriformis*, GenBank accession AJ251772), it available  
431 thus far too little information on the occurrence of membrane-bound  $H^+$ -PPases and  
432 their physiological role in these Protozoa (Pérez-Castiñeira *et al.* 2001). Although  
433 acidocalcisomes as a whole and some of their transport activities have not been  
434 characterized in ciliates as yet, where they may also occur (Plattner *et al.* 2012). In this  
435 study it is clearly evident that the  $H^+$ -PPase in *P. dicentrarchi* colocalises both  
436 phagocytic vacuoles and in the alveolar sacs, and these two structures are acidic cellular  
437 components which are stained with the pH sensitive dye LysoTracker Red DND 99.

438         Although subcellular localization of members of the  $H^+$ -PPase family is mainly  
439 in endocellular membranes (vacuolar tonoplast) and acidocalcisomal membranes of  
440 eukaryotes (algae, plants and protozoa) (Maeshima, 2000; Drozdowicz and Rea, 2001;  
441 Docampo *et al.* 2005) and plasma membrane invaginations of both bacteria and archaea  
442 (Baltscheffsky *et al.* 1999; Serrano *et al.* 2004), evidence for a differential subcellular  
443 localization of the AVP1 (vacuole) and AVP2 (Golgi complex and lysosomes) isoforms  
444 has been only reported in plant cells (Rea *et al.* 1992; Mitsuda *et al.* 2001). Indirect  
445 immunofluorescence microscope with polyclonal antibodies to investigate the

446 subcellular localization of V-H<sup>+</sup>-PPase in *P. falciparum* indicated that VP1 is present  
447 within the vacuolar membrane and, possibly, in food vacuoles (Luo *et al.* 1999;  
448 MacIntosh *et al.* 2001) and it seems that the proton pumps V-H<sup>+</sup>-PPase and V-H<sup>+</sup>-  
449 ATPase are colocalized in acidic organelles in malarian parasites including  
450 acidocalciomes and food vacuoles (Marchesini *et al.* 2000; Saliba *et al.* 2003;  
451 Moriyama *et al.* 2003). In our study, we demonstrate by immunofluorescence and  
452 immunohistochemistry to TEM that the PAB<sub>HK</sub> sera, which recognizes the highly  
453 conserved domain HKAAVIDTIGDPKDT, It generates a specific labeling only on the  
454 alveolar sacs of ciliates, which suggests that this domain is not found, or not recognized  
455 in the H<sup>+</sup>-PPase vacuoles. Thus, immunostaining with PAB<sub>HK</sub> could be evidencing the  
456 possible existence of two isoforms of H<sup>+</sup>-PPase in *P. dicentrarchi*.

457 The existence of multiple H<sup>+</sup>-PPases isoforms is clearly demonstrated in plants  
458 (Venter *et al.* 2006). Thus for example, in rice (*Oryza sativa* L.) genome have been  
459 detected at least two genes encoding the H<sup>+</sup>-PPase (Sakakibara *et al.* 1995), three  
460 isoforms in tobacco (Lerchl *et al.* 1995), two isoforms in red beet (*Beta vulgaris* L.)  
461 (Kim *et al.* 1994), two isoforms in barley (*Hordeum vulgare* L.) (Fukuda *et al.* 2004),  
462 two isoforms in grapevine (*Vitis vinifera* L.) (Venter *et al.* 2006), two isoforms in cacao  
463 (*Theobroma cacao* L.) (Motamayor *et al.* 2013), with highly homologous within the  
464 coding region but differs strongly in the untranslated regions and their expression are  
465 probably regulated in a different manner (Maeshima, 2000). Plants have two  
466 phylogenetically distinct V-H<sup>+</sup>-PPases that can be classified into two subclasses, AVP1,  
467 that depend on cytosolic K<sup>+</sup> for their activity and are moderately sensitive to inhibition  
468 by Ca<sup>2+</sup> and AVP2, which are K<sup>+</sup>-independent but extremely Ca<sup>2+</sup>-sensitive (Sarafian *et*  
469 *al.* 1992; Drozdowicz *et al.* 2000; Gaxiola *et al.* 2007). Parasites, such as in the  
470 malarian parasite *Plasmodium falciparum*, also two genes encoding corresponding VP1

471 and VP2 have been identified (MacIntosh *et al.* 2001), and in ciliates also available in  
472 the databases of the sequence corresponding to an isoform 2 of himenostomatid  
473 *Tetrahymena pyriformis* (GenBank accession AJ251471).

474 There is a near-complete conservation between AVP1/AVP2 of the aminoacids  
475 sequences recognized by polyclonal antibody PAB<sub>HK</sub> (HKAAVIGDTIGPLK) that  
476 provides further justification for the proposal that these antibodies are universal reagents  
477 for the detection of V-PPase polypeptides (Drozdowicz and Rea, 2001). We have  
478 previously shown that H<sup>+</sup>-PPase of *P. dicentrarchi* showed a common motif with the  
479 polyclonal antibody PAB<sub>HK</sub> specific to AVP1 (Mallo *et al.* 2015). Specifically, in this  
480 study we found that this motif is encoded by a gene containing an intercalated  
481 nucleotide sequence to be transcribed into RNA generates two isoforms: one of which  
482 produces a protein with the fragmented motif and other isoform produces a protein  
483 containing the complete motif. The total sizes of the proteins produced by gene  
484 isoforms would vary between 62-64 kD (2kD difference is the estimated size of the  
485 peptide intercalated between the motif PAB<sub>HK</sub>), but an analysis by SDS-PAGE or  
486 Western blot probably would go unnoticed due to the limitation of this technique for  
487 separating proteins of molecular sizes very close (Dauly *et al.* 2006). The hypothesis  
488 proposed in this paper to explain the presence of the two H<sup>+</sup>-PPase isoforms is based, on  
489 the one hand in the differential recognition of the H<sup>+</sup>-PPase in the alveolar sacs by  
490 PAB<sub>HK</sub> antibodies, and secondly, in the presence of two amino acid sequences in the  
491 cDNAs generated by RT-PCR with primers FPiPh / RPiPh. The presence of the two  
492 isoform containing the complete PAB<sub>HK</sub> motif in the H<sup>+</sup>-PPase in the alveolar sacs  
493 could be explained by the existence of an alternative splicing, while isoform 1 of H<sup>+</sup>-  
494 PPase present in the vacuoles not suffer this process and generate a protein with  
495 fragmented motif it would not be recognized by the polyclonal anti-

496 HKAAVIGDTIGPLKDT (PAB<sub>HK</sub>). There are some examples of genes that generate  
497 isoforms transcribed from alternate promoter sites within the gen which may mediate  
498 cell signaling and induce their translocation to various cellular localizations (Saito *et al.*  
499 2002). Furthermore, it is also well known that the splicing regulation can be modulated  
500 by several sequence elements in both exons and introns that either activate (exonic  
501 splicing enhancer, ESE; intronic splicing enhancer, ISE), or repress (exonic splicing  
502 silencer, ESS; intronic splicing silencer, ISS) (Poulos *et al.* 2011).

503 The description of nucleotide sequences of H<sup>+</sup>-PPase genes from plants, bacteria  
504 and archaea brought forward an unusually high degree of sequence conservation  
505 (Serrano *et al.* 2007). In our study, we also found a high level of sequence conservation  
506 of the H<sup>+</sup>-PPase gene among several isolates of *P. dicentrarchi* which also could also be  
507 used, conjunction with other highly conserved genes such as the  $\alpha$ -tubulin, for  
508 detecting intraspecific genetic variation within populations of scuticociliates that infect  
509 cultured turbot (Budiño *et al.* 2011).

510 In plants, it is well established that the efficient exclusion of Na<sup>+</sup> excess from  
511 the cytoplasm and vacuolar Na<sup>+</sup> accumulation are the most important steps towards the  
512 maintenance of ion homeostasis inside the cell, and both tonoplast and plasma  
513 membrane Na<sup>+</sup>/H<sup>+</sup> antiporters exclude Na<sup>+</sup> from the cytosol driven by the H<sup>+</sup>-motive  
514 force generated by the plasma membrane H<sup>+</sup>-ATPase and H<sup>+</sup>-PPase (Silva and Gerós,  
515 2009). Algal and plant H<sup>+</sup>-PPases are induced under anoxia, chilling and salt stresses  
516 (Carystinos *et al.* 1995; Fukuda *et al.* 2004), and overexpression of the vacuolar H<sup>+</sup>-  
517 PPase isoform AVP1 in the model plant *Arabidopsis* has been claimed to confer  
518 increased saline and drought tolerance (Gaxiola *et al.* 2001). Ciliates are eurihalins  
519 organisms particularly well adapt to salinity changes, can live in salinities as low as  
520 4‰ and as high as 62‰ (27‰ higher than seawater) (Hu, 2014). In our study, we found

521 that *P. dicentrarchi* is able to respond to salinity stress with changes in the expression of  
522 H<sup>+</sup>-PPase located in the alveolar sacs indicating a potential role of these structures in  
523 salt tolerance by marine scuticociliates.

524 In conclusión, the H<sup>+</sup>-PPase of *P. dicentrarchi* is located in the membranes of  
525 the phagocytic vacuole and alveolar sacs promoting the acidification of these cellular  
526 compartments. Specifically, in the alveolar sacs are located a isoform of ionic pump H<sup>+</sup>-  
527 PPase containing a highly conserved aa motif generated by alternative splicing process,  
528 that is recognized by polyclonal antibodies PAB<sub>HK</sub>, and whose gene expression is  
529 regulated under conditions altered salt, which suggest that these structures must play an  
530 important physiological role in the adaptative responses of these marine ciliates to  
531 maintenance of both intracellular pH homeostasis and osmoregulation.

532

#### 533 ACKNOWLEDGEMENTS

534 This study was financed by a project from the Ministerio de Economía y  
535 Competitividad (Spain) under grant agreement No. AGL 2014-57125-R, by a project  
536 from the European Union Horizon 2020 research and innovation programme under  
537 grant agreement No. 634429, and by a project from the Xunta de Galicia (Spain) under  
538 grant agreement No. GPC 2014/069.

539

540



## 541 REFERENCES

- 542 **Allen, R.D. and Fok, A.K.** (1983). Nonlysosomal vesicles (acidosomes) are involved  
543 in phagosome acidification in *Paramecium*. *The Journal of Cell Biology* **97**, 566-  
544 570.
- 545 **Baltscheffsky, H., von Stedingk, L.-V., Heldt, H.W. and Klingenberg, M.** (1966).  
546 Inorganic pyrophosphate formation in bacterial photophosphorylation. *Science*  
547 **153**, 1120-1122.
- 548 **Baltscheffsky, M., Schultz, A. and Baltscheffsky, H.** (1999). H<sup>+</sup>-PPases a tightly  
549 membrane-bound family. *FEBS Letters* **457**, 527-533.
- 550 **Belogurov, G.A. and Lahti, R.** (2002). A lysine substitute for K<sup>+</sup>. *Journal of Biological*  
551 *Chemistry* **277**, 49651-49654.
- 552 **Bordier, C.** (1981). Phase separation of integral membrane proteins in Triton X-  
553 114 solution. *Journal of Biological Chemistry* **256**, 1604-1607.
- 554 **Budiño, B., Lamas, J., Pata, M.P., Arranz, J.A., Sanmartín, M.L. and Leiro, J.**  
555 (2011). Intraspecific variability in several isolates of *Philasterides dicentrarchi*  
556 (syn. *Miamiensis avidus*), a scuticociliate parasite of farmed turbot. *Veterinary*  
557 *Parasitology* **175**, 260-272.
- 558 **Bustin, S.A., Benes, V., Garson, J.A., Hellemans, J., Huggett, J., Kubista, M.,**  
559 **Mueller, R., Nolan, T., Pfaffl, M.W., Shipley, G.L., Vandesompele, J. and**  
560 **Wittwer, C.T.** (2009). The MIQE guidelines: minimum information for  
561 publication of quantitative real-time PCR experiments. *Clinical Chemistry* **55**,  
562 611-622.
- 563 **Carystinos, G.D., McDonald, H.R., Monroy, A.F., Dhindsa, R.S. and Poole, R.J.**  
564 (1995). Vacuolar H<sup>+</sup>-translocating pyrophosphatase is induced by anoxia or  
565 chilling in seedlings of rice. *Plant Physiology* **108**, 641-649.

- 566 **Dauly, C., Perlman, D.H., Costello, C.E. and McComb, M.E.** (2006). Protein  
567 separation and characterization by np-RP-HPLC followed by intact MALDI-  
568 TOF mass spectrometry and peptide mass mapping analyses. *Journal of*  
569 *Proteome Research* **5**, 1688-1700.
- 570 **Docampo, R., de Souza, W., Miranda, K., Rohloff, P. and Moreno, S.N.** (2005).  
571 Acidocalcisomes - conserved from bacteria to man. *Nature Reviews*  
572 *Microbiology* **3**, 251-261.
- 573 **Docampo, R., Ulrich, P., Moreno, S.N.J.** (2010). Evolution of acidocalcisomes and  
574 their role in polyphosphate storage and osmoregulation in eukaryotic microbes.  
575 *Philosophical Transactions of Royal Society B* **365**, 775-784.
- 576 **Drozdowicz, Y.M., Kissinger, J.C. and Rea, P.A.** (2000). AVP2, a sequence-  
577 divergent,  $K^+$  insensitive  $H^+$ -translocating inorganic pyrophosphatase from  
578 *Arabidopsis*. *Plant Physiology* **123**, 353-362.
- 579 **Drozdowicz, Y.M. and Rea, P.A.** (2001). Vacuolar  $H^+$  pyrophosphatases: from the  
580 evolutionary backwaters into the mainstream. *Trends in Plant Science* **6**, 206-  
581 211.
- 582 **Drozdowicz, Y.M., Shaw, M., Nishi, M., Striepen, B., Liwinski, H.A., Roos, D.S.**  
583 **and Rea, P.A.** (2003). Isolation and characterization of TgVP1,  
584 a type I vacuolar  $H^+$ -translocating pyrophosphatase from *Toxoplasma gondii*.  
585 The dynamics of its subcellular localization and the cellular effects of a  
586 diphosphonate inhibitor. *The Journal of Biological Chemistry* **278**, 1075-1085.
- 587 **Felsenstein, J.** (1985). Confidence limits on phylogenies: and approach using the  
588 bootstrap. *Evolution* **39**, 783-791.
- 589 **Fukuda, A., Chiba, K., Maeda, M., Nakamura, A., Maeshima, M., Tanaka, Y.**  
590 (2004). Effect of salt and osmotic stresses on the expression of gene for the

- 591 vacuolar H<sup>+</sup>-pyrophosphatase, H<sup>+</sup>-ATPase subunit A, and Na<sup>+</sup>/H<sup>+</sup> antiporter from  
592 barley. *Journal of Experimental Botany* **55**, 585-594.
- 593 **Gaxiola, R.A., Li, J., Undurraga, S., Dang, L.M., Allen, G., Alper, S.L. and Fink,**  
594 **G.R.** (2001). Drought- and salt-tolerant plants result from overexpression of the  
595 AVP1 H<sup>+</sup>-pump. *Proceedings of the National Academy of Sciences USA* **98**,  
596 11444-11449.
- 597 **Gaxiola, R.A., Palmgren, M.G. and Schumacher, K.** (2007). Plant proton pumps.  
598 *FEBS Letters* **581**, 2204-2214.
- 599 **Harper, J.M., Huynh, M.H., Coppens, I., Parussini, F., Moreno, S., Carruthers,**  
600 **V.B.** (2006). A cleavable propeptide influences *Toxoplasma* infection by  
601 facilitating the trafficking and secretion of the TgMIC2-M2AP invasion  
602 complex. *Molecular Biology of the Cell* **17**, 4551–4563.
- 603 **Hu, X.** (2014). Ciliates in extreme environments. *Journal of Eukaryotic Microbiology* **61**,  
604 410-418.
- 605 **Iglesias, R., Paramá, A., Álvarez, M.F., Leiro, J., Fernández, J. and Sanmartín,**  
606 **M.L.** (2001) *Philasterides dicentrarchi* (Ciliophora, Scuticociliatida) as the  
607 causative agent of scuticociliatosis in farmed turbot *Scophthalmus maximus* in  
608 Galicia (NW Spain). *Diseases of Aquatic Organisms* **46**, 47-55.
- 609 **Iglesias, R., Paramá, A., Álvarez, M.F., Leiro, J., Aja, C. and Sanmartín, M.L.**  
610 (2003). *In vitro* growth requirements for the fish  
611 pathogen *Philasterides dicentrarchi* (Ciliophora, Scuticociliatida). *Veterinary*  
612 *Parasitology* **111**:19-30.
- 613 **Ito, H., Fukuda, Y., Murata, K. and Kimura, A.** (1983). Transformation of intact  
614 yeast cells treated with alkali cations *Journal of Bacteriology* **153**, 163–168

- 615 **Karlsson, J.** (1975). Membrane-bound potassium and magnesium ion-stimulated  
616 inorganic pyrophosphatase from roots and cotyledons of sugar beet (*Beta*  
617 *vulgaris* L.). *Biochimica et Biophysica Acta* **399**, 356-363.
- 618 **Kim, Y., Kim, E.J. and Rea, P.A.** (1994). Isolation and characterization of cDNAs  
619 encoding the vacuolar H<sup>+</sup>-pyrophosphatase of *Beta vulgaris*. *Plant Physiology*  
620 **106**, 375-382.
- 621 **Kimura, M.** (1980). A simple method for estimating evolutionary rates of base  
622 substitutions through comparative studies of nucleotide sequences. *Journal of*  
623 *Molecular Evolution* **16**, 111-120.
- 624 **Lerchl, J., König, S., Zrenner, R. and Sonnewald, U.** (1995). Molecular cloning,  
625 characterization and expression of isoforms encoding tonoplast-bound proton-  
626 translocating inorganic pyrophosphatase in tobacco. *Plant Molecular Biology* **28**,  
627 833-840.
- 628 **Livak, K.J. and Schmittgen, T.D.** (2001). Analysis of relative gene expression data  
629 using real-time quantitative PCR and the 2<sup>- $\Delta\Delta C_T$</sup>  Method. *Methods* **25**, 402-408.
- 630 **Long, A.R., Williams, L.E., Nelson, S.J. and Hall, J.L.** (1995). Localization of  
631 membrane pyrophosphatase activity in *Ricinus communis* seedlings. *Journal of*  
632 *Plant Physiology* **146**, 629-638.
- 633 **López-López, O., Fuciños, P., Pastrana, L., Rúa, M.L., Cerdán, M.E. and**  
634 **González-Siso, M.I.** (2010). Heterologous expression of an esterase from  
635 *Thermus thermophilus* HB27 in *Saccharomyces cerevisiae*. *Journal of*  
636 *Biotechnology* **145**, 226-232.
- 637 **Luo, S., Marchesini, N., Moreno, S.N. and Docampo, R.** (1999). A plant-like vacuolar  
638 H(+)-pyrophosphatase in *Plasmodium falciparum*. *FEBS Letters* **460**, 217-220.

- 639 **Maeshima, M.** (2000). Vacuolar H<sup>+</sup>-pyrophosphatase. *Biochimica et Biophysica Acta*  
640 **1465**, 37-51.
- 641 **Mallo, N., Lamas, J. and Leiro, J.M.** (2013). Evidence of an alternative oxidase  
642 pathway for mitochondrial respiration in the scuticociliate *Philasterides*  
643 *dicentrarchi*. *Protist* **164**, 824-836.
- 644 **Mallo, N., Lamas, J., Piazzon, C. and Leiro, J.M.** (2015). Presence of a plant-like  
645 proton-translocating pyrophosphatase in a scuticociliate parasite and its role as a  
646 possible drug target. *Parasitology* **142**, 449-462.
- 647 **Marchesini, N., Luo, S., Rodrigues, C.O., Moreno, S.N.J. and Docampo, R.** (2000).  
648 Acidocalcisomes and vacuolar H<sup>+</sup>-pyrophosphatase in malaria parasites.  
649 *Biochemical Journal* **347**, 243-253.
- 650 **MacIntosh, M.T., Drozdowicz, Y.M., Laroiya, K., Rea, P.A. and Vaidya, A.B.**  
651 (2001). Two classes of plant-like vacuolar-type H<sup>(+)</sup>-pyrophosphatases in  
652 malaria parasites. *Molecular and Biochemical Parasitology* **114**, 183-195.
- 653 **Mitsuda, N., Enami, K., Nakata, M., Takeyasu, K. and Sato, M.H.** (2001). Novel  
654 type *Arabidopsis thaliana* H<sup>+</sup>-PPase is localized to the Golgi apparatus. *FEBS*  
655 *Letters* **488**, 29-33.
- 656 **Moreno, S.N.J. and Docampo, R.** (2009). The role of acidocalcisomes in parasitic  
657 protists. *Journal of Eukaryotic Microbiology* **56**, 208-213.
- 658 **Moriyama, Y., Hayashi, M., Yatsushiro, S. and Yamamoto, A.** (2003).  
659 Vacuolar proton pumps in malaria parasite cells. *Journal of Bioenergetics and*  
660 *Biomembranes* **35**: 367-375.
- 661 **Motamayor, J.C., Mockaitis, K., Schmutz, J., Haiminen, N., Livingstone,**  
662 **D., Cornejo, O., Findley, S.D., Zheng, P., Utro, F., Royaert, S., Sasaki,**  
663 **C., Jenkins, J., Podicheti, R., Zhao, M., Scheffler, B.E., Stack, J.C., Feltus,**

- 664 F.A., Mustiga, G.M., Amores, F., Phillips, W., Marelli, J.P., May,  
665 G.D., Shapiro, H., Ma, J., Bustamante, C.D., Schnell, R.J., Main,  
666 D., Gilbert, D., Parida, L. and Kuhn, D.N. (2013) The genome sequence of the  
667 most widely cultivated cacao type and its use to identify candidate genes  
668 regulating pod color. *Genome Biology* **14**, r53.
- 669 Pérez-Castiñeira, J.R., Gómez-García, R., López-Marqués, R.L., Losada, M. and  
670 Serrano, A. (2001) Enzymatic systems of inorganic pyrophosphatase  
671 bioenergetics in photosynthetic and heterotrophic protists: remnants or metabolic  
672 cornerstones? *International Microbiology* **4**, 135-142.
- 673 Pérez-Castiñeira, J.R., Alvar, J., Ruiz-Pérez, L.M. and Serrano, A. (2002).  
674 Evidence for a wide occurrence of proton-translocating pyrophosphatase genes  
675 in parasitic and free-living protozoa. *Biochemical and Biophysical Research*  
676 *Communications* **294**, 567-573.
- 677 Philimonenko, V.V., Janáček, J. and Hozák, P. (2002). LR White is preferable to  
678 Unicryl for immunogold detection of fixation sensitive nuclear antigens.  
679 *European Journal of Histochemistry* **46**, 359-364.
- 680 Piazzón, C., Lamas, J., Castro, R., Budiño, B., Cabaleiro, S., Sanmartín, M.L.  
681 and Leiro, J. (2008). Antigenic and cross-protection studies on two turbot  
682 scuticociliate isolates. *Fish and Shellfish Immunology* **25**, 417-424.
- 683 Piazzon, C., Lamas, J. and Leiro, J.M. (2011). Role of scuticociliate proteinases in  
684 infection success in turbot, *Psetta maxima* (L.). *Parasite Immunology* **33**, 535-  
685 544.
- 686 Plattner, H., Sehring, I.M., Mohamed, I.K., Miranda, K., De Souza, W., Billington,  
687 R., Genazzani, A. and Ladenburger, E.M. (2012) Calcium signaling in closely  
688 related protozoan groups (Alveolata): non-parasitic ciliates (*Paramecium*,

- 689 *Tetrahymena*) vs. parasitic Apicomplexa (*Plasmodium*, *Toxoplasma*). *Cell*  
690 *Calcium* **51**, 351-382.
- 691 **Poulos, M.G., Batra, R., Charizanis, K. and Swanson, M.S.** (2011). Developments in  
692 RNA splicing and disease. *Cold Spring Harbor Perspectives in Biology* **3**,  
693 a000778.
- 694 **Rea, P.A. and Poole, R.J.** (1993). Vacuolar H<sup>+</sup>-translocating pyrophosphatase. *Annual*  
695 *Review of Plant Physiology and Plant Molecular Biology* **44**, 157-180.
- 696 **Rea, P.A., Kim, Y., Sarafian, V., Poole, R.J., Davies, J.M. and Sanders, D.** (1992).  
697 Vacuolar H<sup>+</sup>-translocating pyrophosphatases: a new category of ion translocase.  
698 *Trends in Biochemical Sciences* **17**, 348-353.
- 699 **Robinson, D.G., Haschke, H.P., Hinz, G., Hoh, B., Maeshima, M. and Marty, F.**  
700 (1996). Immunological detection of tonoplast polypeptides in the plasma  
701 membrane of pea cotyledons. *Planta* **198**, 95-103.
- 702 **Saitoh, O., Murata, Y., Odagiri, M., Itoh, M., Itoh, H., Misaka, T. and Kubo, Y.**  
703 (2002). Alternative splicing of RGS8 gene determines inhibitory function of  
704 receptor type-specific Gq signaling. *Proceedings of the National Academy of*  
705 *Sciences USA* **99**, 10138-10143.
- 706 **Saliba, K.J., Allen, R.J., Zisis, S., Bray, P.G., Ward, S.A. and Kirk, K.** (2003).  
707 Acidification of the malaria parasite's digestive vacuole by a H<sup>+</sup>-ATPase and a  
708 H<sup>+</sup>-pyrophosphatase. *The Journal of Biological Chemistry* **278**, 5605-5612.
- 709 **Sarafian, V., Kim, Y., Poole, R.J. and Rea, P.A.** (1992). Molecular cloning and  
710 sequence of cDNA encoding the pyrophosphate-energized vacuolar membrane  
711 proton pump of *Arabidopsis thaliana*. *Proceedings of the National Academy of*  
712 *Sciences USA* **89**, 1775-1779.

- 713 **Scott, D.A. and Docampo, R.** (2000). Characterization of isolated acidocalcisomes of  
714 *Trypanosoma cruzi*. *The Journal of Biological Chemistry* **275**, 24215-24221.
- 715 **Serrano, A., Pérez-Castiñeira, R., and Baltscheffsky, H.** (2004). Proton-pumping  
716 inorganic pyrophosphatases in some archea and other extremophilic prokaryotes.  
717 *Journal of Bioenergetics and Biomembranes* **36**, 127-133.
- 718 **Serrano, A, Pérez-Castiñeira, J.R., Baltscheffsky, M. And Baltscheffsky, H.** (2007).  
719  $H^+$ -PPases: yesterday, today and tomorrow. *IUBMB Life* **59**, 76-83.
- 720 **Sievers, F., Wilm, A., Dineen, D., Gibson, T.J., Karplus, K., Li, W., López, R.,**  
721 **McWilliam, H., Remmert, M., Söding, J., Thompson, J.D. and Higgins, D.G.**  
722 (2011). Fast, scalable generation of high-quality protein multiple sequence  
723 alignments using Clustal Omega. *Molecular Systems Biology* **7**, 539.
- 724 **Silva, P. and Gerós, H.** (2009). Regulation by salt of vacuolar  $H^+$ -ATPase and  $H^+$ -  
725 pyrophosphatase activities and  $Na^+/H^+$  Exchange. *Plant Signaling and Behavior*  
726 **4**, 718-726.
- 727 **Scott, D.A., de Souza, W., Benchimol, M., Zhong, I., Lu, H.G., Moreno, S.N. and**  
728 **Docampo, R.** (1998). Presence of a plant-like proton-pumping pyrophosphatase  
729 in acidocalcisomes of *Trypanosoma cruzi*. *The Journal of Biological Chemistry*  
730 **273**, 22151-22158.
- 731 **Sakakibara, Y., Kobayashi, H. and Kasamo, K.** (1996). Isolation and characterization  
732 of cDNAs encoding vacuolar  $H^+$ -pyrophosphatase isoforms from rice (*Oryza*  
733 *sativa* L.). *Plant Molecular Biology* **31**, 1029-1038.
- 734 **Tamura, K., Stecher, G., Peterson, D., Filipski, A. and Kumar, S.** (2013). MEGA6:  
735 Molecular Evolutionary Genetics Analysis version 6.0. *Molecular Biology and*  
736 *Evolution* **30**, 2725-2729.



737 **Venter, M., Gronewald, J.-H. and Botha, F.C.** (2006). Sequence analysis and  
738 transcriptional profiling of two vacuolar H<sup>+</sup>-pyrophosphatase isoforms in *Vitis*  
739 *vinifera*. *Journal of Plant Research* **119**, 469-478.

740

741

For Peer Review

## 742 FIGURE LEGENDS

743

744 **Figure 1.** A, B ) Immunofluorescence detection by confocal microscopy of H<sup>+</sup>-PPase in  
745 a ciliate trophozoite using a mouse antibody anti- recombinant H<sup>+</sup>-PPase expressed in  
746 yeast *Saccharomyces cerevisiae* and a secondary polyclonal antibody anti-mouse Ig  
747 conjugated with FITC. After immunofluorescence assay, trophozoites were  
748 counterstained with DAPI to identify the macronucleus (M). A) Arrows indicate the  
749 immunolocalization of H<sup>+</sup>-PPase in the vacuoles and arrowhead indicate the presence of  
750 a specific immunostaining appears as a dotted line coinciding with the alveolar sacs. B)  
751 Fluorescent staining of acidic compartments of *P. dicentrarchi* using LysoTracker Red  
752 DND-99 show a fluorescent staining of the posterior vacuoles (arrows) and the alveolar  
753 sacs (arrowhead). Scale bars = 10 μm.

754

755 **Figure 2.** Immunofluorescence detection by confocal microscopy of H<sup>+</sup>-PPase isoform  
756 (H<sup>+</sup>-PPase2) with PAB<sub>HK</sub> polyclonal antibody (A) and anti-AVP1 polyclonal antisera  
757 (B) where you can see a pattern of discontinuous fluorescence on the surface of  
758 trophozoites (arrowhead). C,D) Immunoelectromicroscopy localization of the isoform  
759 H<sup>+</sup>-PPase2 using the polyclonal PAB<sub>HK</sub> antibody corresponding to AVP1 isoform of *A.*  
760 *thaliana* and which shows a specific staining (arrowhead) on the membrane of the  
761 alveolar sacs.

762

763 **Figure 3.** A) Nucleotide sequence belonging to a gene region of the H<sup>+</sup>-PPase of *P.*  
764 *dicentrarchi* together with its corresponding translation into amino acids, containing a  
765 sequence motif recognized by the antibody PAB<sub>HK</sub> (box in black). In the lower part of  
766 the figure are shown the products of PCR and RT-PCR obtained using ADN and RNA

767 as template and the primers FPiPh/RPiPh, analyzed on agarose gel 4% being observed  
768 in the case of using cDNA as template, the presence of two bands that correspond,  
769 respectively to isoform 1 (the larger), and 2 (the smallest) and containing this last the  
770 complete motif recognized by the polyclonal antibody PAB<sub>HK</sub>. B) Western blot with  
771 antibody PAB<sub>HK</sub> (lane 1) on ciliate membrane-associated proteins (MAPs) of  
772 trophozoites subjected to SDS-PAGE under nonreducing conditions and which  
773 recognizes a single band of approximately 62 kD (arrow). Mw: Molecular weight  
774 markers.

775

776 **Figure 4.** A) Multiple sequence alignment using Clustal Omega program of aa  
777 sequences obtained from a partial ORF of the gene of H<sup>+</sup>-PPasa from several isolates  
778 (B<sub>1</sub>, D<sub>2</sub>, D<sub>3</sub>, C<sub>1</sub>, I<sub>1</sub>, S<sub>1</sub> y P<sub>1</sub>) of *P. dicentrarchi*. The boxes in bold indicate the motif  
779 recognized by the antibody PAB<sub>HK</sub>. B) Phylogenetic comparison of H<sup>+</sup>-PPase of *P.*  
780 *dicentrarchi* isolates. Aligned Aa sequences were subjected to phylogenic analysis with  
781 neighbor joining (NJ) method. The numbers at the nodes represent bootstrap values out  
782 of 1000 resampled values in the NJ analysis with the Kimura two-parameter correction  
783 model.

784

785 **Figure 5.** Relative gene expression levels of H<sup>+</sup>-PPase of *P. dicentrarchi* determined by  
786 RT-qPCR in trophozoites incubated for 24 h in medium containing different  
787 concentrations of NaCl: 4, 8 and 37 ‰. Gene expression was normalized to reference  
788 gene  $\alpha$ -tubulin of *P. dicentrarchi* and normalized data are expressed in arbitrary units.  
789 Values shown are means  $\pm$  standard error (E.S.) of five assays. \**P* < 0.01 relative to  
790 ciliates incubated in the medium containing a salt concentration of 37 ‰.

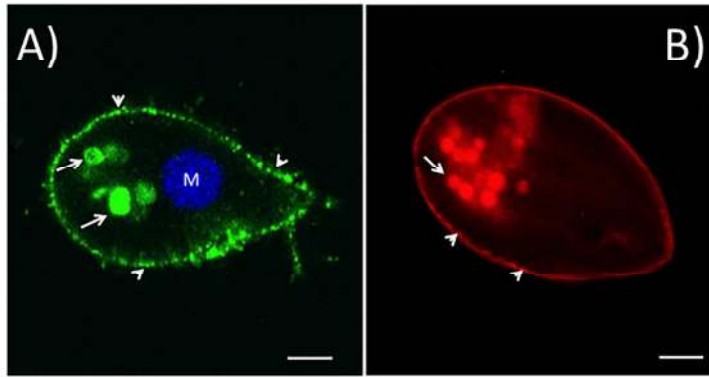


Figure 1

119x90mm (300 x 300 DPI)

Review

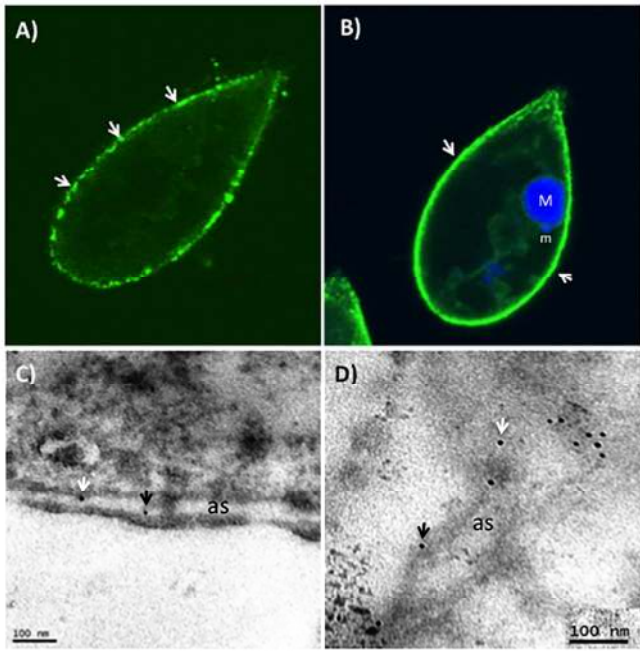


Figure 2

119x90mm (300 x 300 DPI)

Review

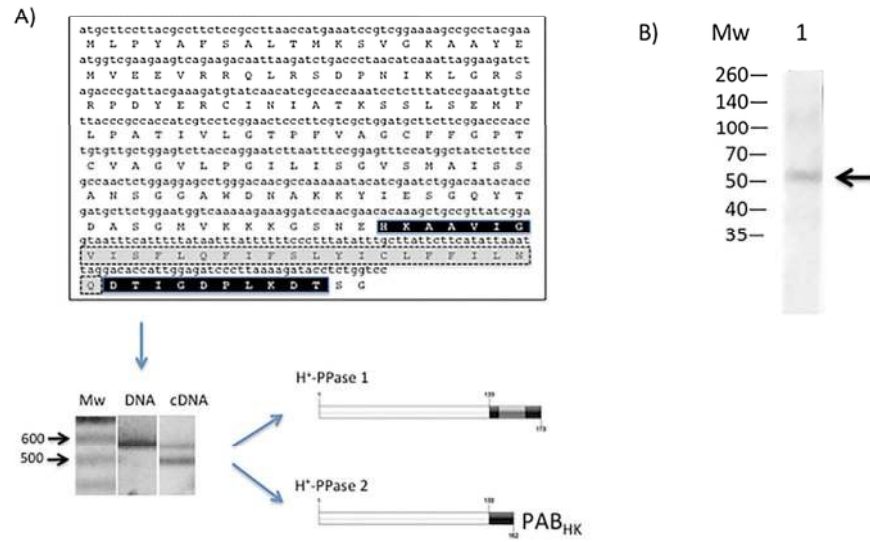


Figure 3

90x67mm (300 x 300 DPI)

A)

```

D2  MLPYAFSALTMKSVGKAAAYEMVEEVRRLRSDPNIKLGRSRPDYERCINIATKSSLSEMF
I1  MLPYAFSALTMKSVGKAAAYEMVEEVRRLRSDPNIKLGRSRPDYERCINIATKSSLSEMF
B1  MLPYAFSALTMKSVGKAAAYEMVEEVRRLRSDPNIKLGRSRPDYERCINIATKSSLSEMF
D3  MLPYAFSALTMKSVGKAAAYEMVEEVRRLRSDPNIKLGRSRPDYERCINIATKSSLSEMF
P1  MLPYAFSALTMKSVGKAAAYEMVEEVRRLRSDPNIKLGRSRPDYERCINIATKSSLSEMF
S1  MLPYAFSALTMKSVGKAAAYEMVEEVRRLRSDPNIKLGRSRPDYERCINIATKSSLSEMF
C1  MLPYAFSALTMKSVGKAAAYEMVEEVRRLRSDPNIKLGRSRPDYERCINIATKSSLSEMF
*****

D2  LPATIVLGTFFVAGCFPGPTCVAGVLPGLISGVSMAISSANSGGAWDNAKKYIESGQYT
I1  LPATIVLGTFFVAGCFPGPTCVAGVLPGLISGVSMAISSANSGGAWDNAKKYIESGQYT
B1  LPATIVLGTFFVAGCFPGPTCVAGVLPGLISGVSMAISSANSGGAWDNAKKYIESGQYT
D3  LPATIVLGTFFVAGCFPGPTCVAGVLPGLISGVSMAISSANSGGAWDNAKKYIESGQYT
P1  LPATIVLGTFFVAGCFPGPTCVAGVLPGLISGVSMAISSANSGGAWDNAKKYIESGQYT
S1  LPATIVLGTFFVAGCFPGPTCVAGVLPGLISGVSMAISSANSGGAWDNAKKYIESGQYT
C1  LPATIVLGTFFVAGCFPGPTCVAGVLPGLISGVSMAISSANSGGAWDNAKKYIESGQYT
*****

D2  DASGMVKKKGSNEBKAAVIIVISFLQIFSLYICLFFILNODTIGDPLKDTSG
I1  DASGMVKKKGSNEBKAAVIIVISFLQIFSLYICLFFILNODTIGDPLKDTSG
B1  DASGMVKKKGSNEBKAAVIIVISFLQIFSLYICLFFILNODTIGDPLKDTSG
D3  DASGMVKKKGSNEBKAAVIIVISFLQIFSLYICLFFILNODTIGDPLKDTSG
P1  DASGMVKKKGSNEBKAAVIIVISFLQIFSLYICLFFILNODTIGDPLKDTSG
S1  DASGMVKKKGSNEBKAAVIIVISFLQIFSLYICLFFILNODTIGDPLKDTSG
C1  DASGMVKKKGSNEBKAAVIIVISFLQIFSLYICLFFILNODTIGDPLKDTSG
*****
    
```

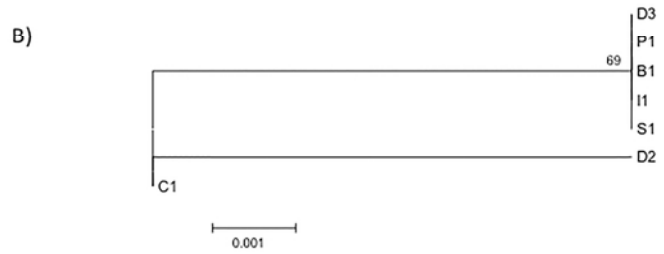


Figure 4

90x67mm (300 x 300 DPI)

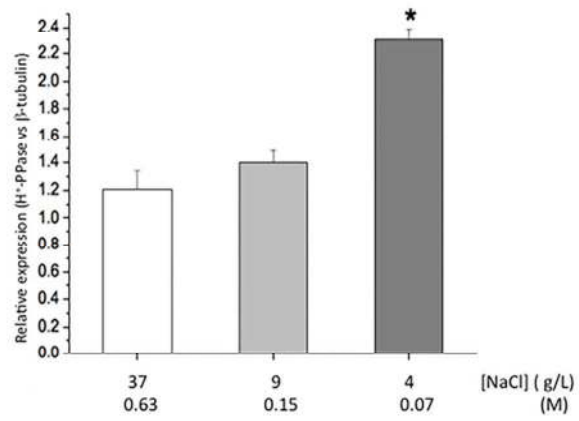


Figure 5

90x67mm (300 x 300 DPI)